

# Electrically induced interactions between colloidal particles in the vicinity of a conducting plane

François Nadal, Françoise Argoul, Patrick Hanusse, and Bernard Pouligny  
*Centre de Recherche Paul Pascal, Avenue Schweitzer, 33600 Pessac, France*

Armand Ajdari

*Laboratoire de Physico-Chimie Théorique, UMR CNRS 7083, ESPCI, 10 rue Vauquelin, 75005 Paris, France*

(Received 7 January 2002; published 25 June 2002)

We address the problem of two-dimensional (2D) colloidal aggregation driven by an ac electrical field, by observing an aqueous dispersion of latex microspheres in contact with a conducting surface. Using micron-sized carboxylated polystyrene particles, we have systematically investigated the aggregation process, as a function of particle size and charge, and of the applied electric field amplitude and frequency. A low-density 2D phase is observed at high frequency (typically above 1 kHz), while at low frequency (below a “contact frequency”  $\nu_c$ ) the collection of particles collapses into disconnected compact aggregates of crystalline (hexagonal) structure. We argue that this scenario is governed by the competition between an attractive force, of electrohydrodynamic nature, and a repulsive force, basically an electrical dipole-dipole interaction. Both contributions are revealed and analyzed in independent experiments on isolated particle pairs, using optical manipulation and dynamometry.

DOI: 10.1103/PhysRevE.65.061409

PACS number(s): 82.70.Dd

## I. INTRODUCTION

The academic and technical interest of the scientific community for colloidal systems and their organization in liquid phases can be traced back to the beginning of the 20th century [1,2]. In many situations, the well-known Deryagin-Landau-Verwey-Overbeek (DLVO) theory [3,4] succeeded in explaining the coagulation or dispersion behaviors of simple colloids. In addition to DLVO colloidal forces, capillary interactions have been shown to promote particle aggregation in two-dimensional (2D) systems [5–9] at equilibrium. Forces of different nature are involved in systems driven far from equilibrium by mechanical, electrical or magnetic forcing. Recent studies have reported self-organization probably due to hydrodynamic (thermoconvective) or electrohydrodynamic effects [10–13]. An earlier work [14] had shown that the aggregation of latex microspheres on a solid surface could also be induced by an ac electric field. This process was later observed with dc electric fields [15]. Three lines of interpretation of this phenomenon have been proposed in the literature so far. The first one, supported by calculations and experimental evidence [12], argued that the attractive force leading to particle aggregation might originate from an electro-osmotic flow due to the surface charge of the particles. This study focused essentially on dc electric fields, and the mechanism proposed cannot be generalized to ac electric fields. The second one [16] stated that the electrohydrodynamic flow producing the aggregation might be due to the particle induced distortion of the applied field (either dc or ac) in the vicinity of the double layer of ions and counterions at the electrode surface. A third one [10] suggested a driving mechanism involving bulk charge densities—resulting from electrode polarization—in inhomogeneous electric fields.

In the present paper, we report complementary experimental evidence that supports the interpretation scheme put

forward by Yeh *et al.* [16]. Focusing on ac electric fields, we propose an original experimental and quantitative survey of the role of the different parameters—amplitude and frequency of the electric field, size and charge of the particles—in the self-organization process. Furthermore, we show that the aggregation mechanism occurs as a continuous transition from a 2D low-density phase at high frequency (typically about 10 kHz) to 2D disconnected compact aggregates (internal hexagonal geometry) below a characteristic frequency  $\nu_c$ , at which the particles come into contact. As a complement to these observations of the many-particle behavior, we report an experimental study of features of the two-particle interaction by means of optical tweezers. From the data, we deduce the strength and scaling behavior of the two opposing forces involved in the aggregation process: a repulsive dipolar force, and an attractive electrohydrodynamic force originating from a rectified electro-osmotic flow along the surface of the conducting plates.

## II. EXPERIMENT SETUP

The sample cell, sketched in Fig. 1, was composed of two parallel horizontal conducting plates (ITO coated glass,  $50 \Omega$  per square, purchased from CRL, UK), separated by a PTFE (polytetrafluoroethane) spacer of thickness  $L=270 \pm 20 \mu\text{m}$  (purchased from Goodfellow, UK). The working electrode surface area was about  $1 \text{ cm}^2$ . The void between the plates was filled with a [1:1] electrolyte ( $\text{NaOH } 10^{-4} \text{ M}$ , Debye length  $\lambda_D=30 \text{ nm}$ ) containing the solid particles: monodisperse carboxylated microspheres (density 1.045) provided by Polyscience (USA) and IDC (Interfacial Dynamics Corporation, USA). We studied particles of different radius  $a$  (between  $0.37 \mu\text{m}$  and  $5 \mu\text{m}$ ), and different surface charge densities (see Table I for particles of about  $1.5 \mu\text{m}$  in radius: the values of  $\zeta$  potentials reported were measured

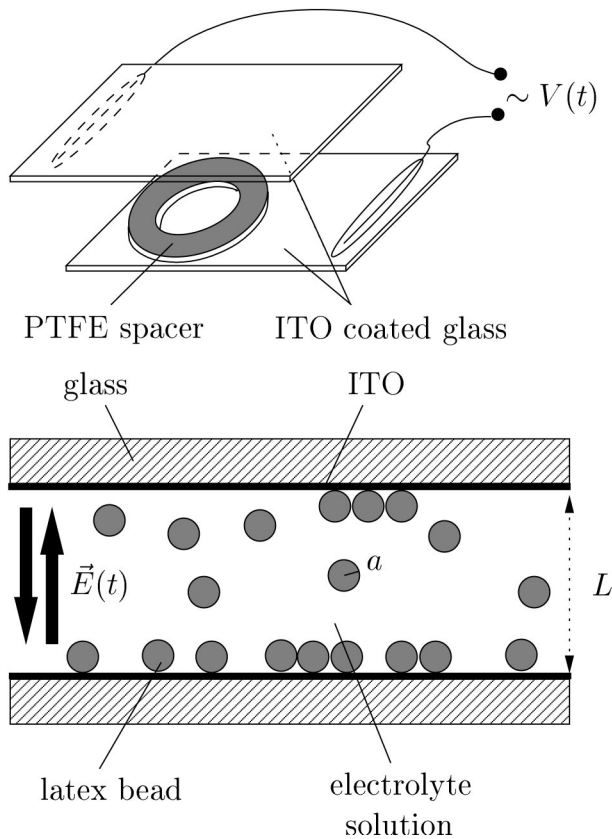


FIG. 1. Sketch of the experimental setup.

using a Malvern  $\zeta$  sizer, while the surface charge values  $\sigma_s$  were provided by IDC).

An electrostatic potential difference  $V(t) = V_o \cos(2\pi\nu t)$ , was applied between the conducting plates.  $V_o$  was varied between 1 and 10 V, corresponding to an average electric field in the 37–370  $\text{V cm}^{-1}$  range. Frequencies  $\nu$  from 50 Hz to 10 kHz were explored.

The particles were observed through a microscope (Olympus BH-2), equipped with a CCD camera (Hamamatsu C5985) and a video recorder (Umatic, SONY VO9850 OP) coupled to a frame grabber (Psion interface driven by a NIH 1.61 Image software) to allow for particle dynamics analysis.

Experiments on isolated particle pairs were carried out by means of a double optical trap setup (see [17] for details). To characterize the dipolar force, a dedicated experiment was

TABLE I. Measured  $\zeta$  potentials of four surface charge calibrated carboxylate particles. In the fourth column are reported the values of the surface charge density  $\sigma_s$  when provided by the supplier.

Radius $a$ ( $\mu\text{m}$ )	Supplier	$\zeta$ (mV)	$\sigma_s$ ( $\mu\text{C cm}^{-2}$ )	$\nu_c$ (kHz)
1.6	IDC	$-51.5 \pm 4.8$	11.9	1.2
1.75	IDC	$-17.8 \pm 3.7$	3.0	1.25
1.75	IDC	$-7.7 \pm 4.8$		1.3
1.5	Polyscience	$-47.2 \pm 5.4$		1.2

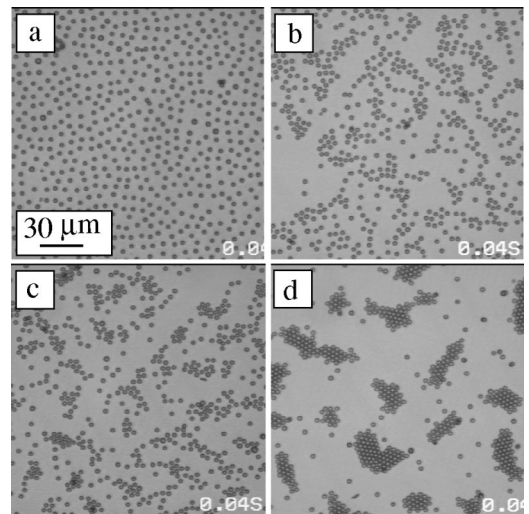


FIG. 2. Stationary patterns on the bottom plate obtained with a dispersion of latex particles,  $a = 1.5 \mu\text{m}$  in diameter, for different frequencies. (a)  $\nu = 2$  kHz, (b)  $\nu = 1.5$  kHz, (c)  $\nu = 1.3$  kHz, (d)  $\nu = 1$  kHz.  $E_o = V_o/L = 185 \text{ V cm}^{-1}$ .

designed using horizontal platinum wires as electrodes (see Fig. 7).

### III. COLLECTIVE BEHAVIOR

The first set of experiments involved a large number of particles (after deposition, roughly one-fifth of the working electrode surface was covered). Prior to varying parameters, we let the particles accumulate on the conducting plates under an ac electric field at frequencies of about 10 kHz. We observed that most particles did deposit on the bottom plate due to sedimentation, but that a minority was trapped just below the top one. This suggests that there exists a strong electrostatic image interaction that attracts the beads onto the walls, and confines them in the  $z$  direction (perpendicular to the electrodes). The image interaction is probably due to the depolarization field of the dielectric bead, which is unscreened as long as the frequency is high enough so that the electrolyte does not reach equilibrium. This attraction seems to be long ranged (a few bead radius), as it definitely increased the particles deposition velocity, as compared to the case where only gravity was acting. While trapped in the  $z$  direction, most particles underwent a free Brownian-like motion in the  $x, y$  directions (parallel to the electrodes). However, we noticed that a few particles were definitely and irreversibly stuck to the electrodes. The confinement of Brownian particles was reversible since these particles did redisperse in the bulk upon cancellation of the electric field.

Once the surfaces had gathered all the beads present (stationary surface fraction of particles on the conducting plates), we focused the microscope on the bottom surface, where most of the beads were located and started varying the electric potential frequency  $\nu$  for different values of  $V_o$ .

Figure 2 shows typical configurations corresponding to different values of the frequency  $\nu$  for a fixed value of  $V_o$ . Observation demonstrated that the particles assemble into

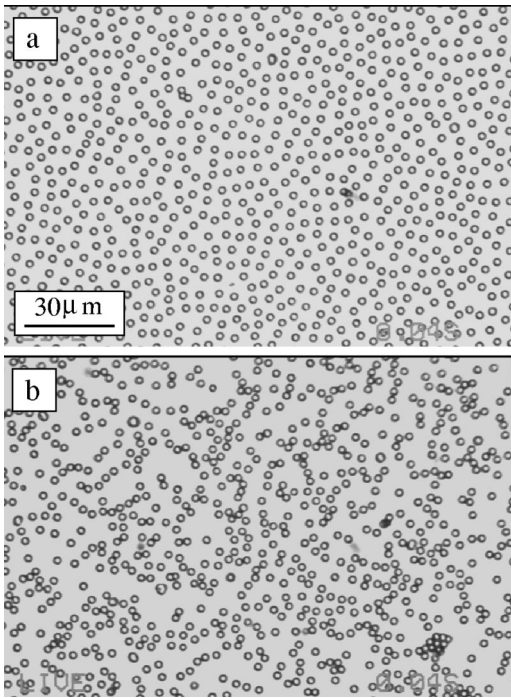


FIG. 3. (a) Structure of an assembly of  $a=1.5 \mu\text{m}$  particles deposited under ac electric field ( $E_o=185 \text{ V cm}^{-1}$  and  $\nu=2 \text{ kHz}$ ). (b) Structure of an assembly of identical particles deposited under gravity field only (without electric field).

packed aggregates (local hexagonal ordering) when  $\nu$  is lower than a characteristic “contact frequency”  $\nu_c$ . The value of  $\nu_c$  was visually determined as the frequency at which the particles got approximately in contact. For frequencies higher than  $\nu_c$  (high frequency or HF regime), the beads were spread in very large patches (about  $1 \text{ mm}^2$ ). Inside these patches, the particles were separated from their nearest neighbors by a characteristic finite distance, of the order of several bead radii [see Fig. 2(a)]. A comparison with the particle distribution in the absence of electric field (an example is shown in Fig. 3) confirms that the distribution of particles in the HF regime is not totally random but looks rather like a thermally blurred hexagonal distribution. When the frequency was decreased towards  $\nu_c$ , the beads got closer to each other. The surface fraction of beads being a conserved quantity, the cell surface divided into “empty” and “covered” zones [Figs. 2(b) and 2(c)]. Below  $\nu_c$  (low frequency or LF regime) crystalline aggregates were formed, the internal density and compacity of which increased as the frequency was decreased. Photographs of such aggregates at three different magnifications are shown in Figs. 4(a)–4(c). The aggregates typical size depended on both the initial density of particles and the electric field parameters. The aggregates are distributed rather uniformly over the cell. The particles remained mobile in the plane of the ITO surface and the aggregation process was checked to be reversible, i.e., as soon as the frequency was turned back from the LF ( $\nu < \nu_c$ ) to the HF ( $\nu > \nu_c$ ) regime, the aggregates “exploded,” evidencing a strong repulsion. After a few minutes, the system was back to a typical HF configuration. By contrast, when the ac electric field at  $\nu < \nu_c$  was simply turned off, the

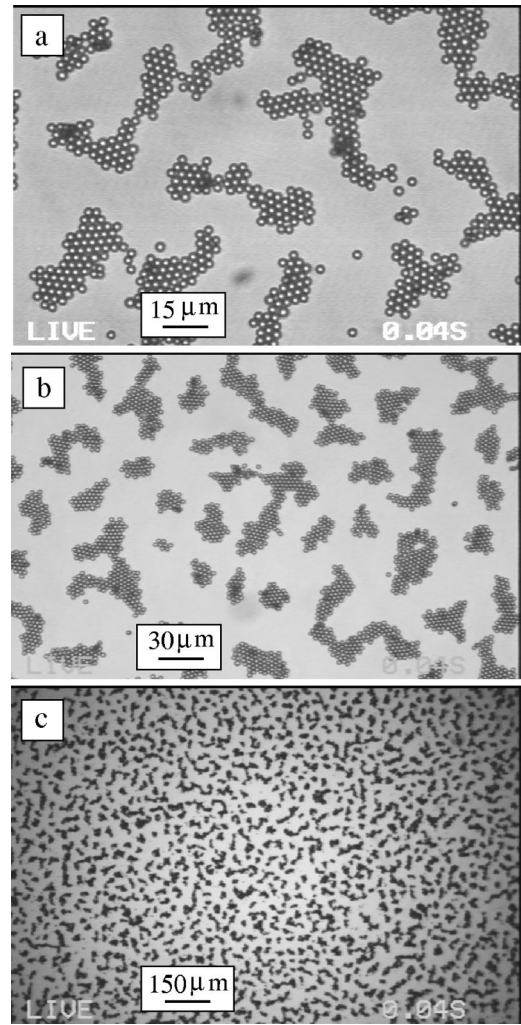


FIG. 4. Images of the aggregated regime for three different magnifications: (a)  $\times 40$ , (b)  $\times 20$ , (c)  $\times 4$ .  $E_o=185 \text{ V cm}^{-1}$ ,  $\nu=400 \text{ Hz}$ ,  $a=1.5 \mu\text{m}$ .

aggregates started melting by diffusion with no clear indication of repulsions.

We have performed a systematic determination of the contact frequency  $\nu_c$ , as a function of  $E_o=V_o/L$  and of the bead radius  $a$ . Note that the “applied field”  $E_o$  may differ from the local electric field in the cell, because of the double-layer polarization at the electrodes. Nevertheless, the cut off frequency of the cell,  $D/\lambda_D L$  [where  $D$  is the mean diffusion coefficient of the ions and counterions in the electrolyte (NaOH), and  $\lambda_D$  the Debye length], is rather low ( $\sim 250 \text{ Hz}$ ) with respect to the range of ac field frequencies used in this study. Therefore, the field in bulk should not deviate too much from  $V_o/L$  for  $\nu \geq 500 \text{ Hz}$ .

To determine  $\nu_c$  with a good precision, we decreased the frequency (at fixed  $V_o$ ) from  $10 \text{ kHz}$  down to  $50 \text{ Hz}$  by small steps ( $\Delta \nu \sim 50\text{--}100 \text{ Hz}$ ), letting the system stabilize at each intermediate frequency. This procedure was repeated for different bead size  $a$ . Figure 5 shows the dependence of  $\nu_c$  as a function of  $a$  for three values of  $V_o$  [Fig. 5(a)] and as a function of  $V_o$  for three values of the particles radius  $a$  [Fig. 5(b)]. The first feature to be noticed is the strong dependence

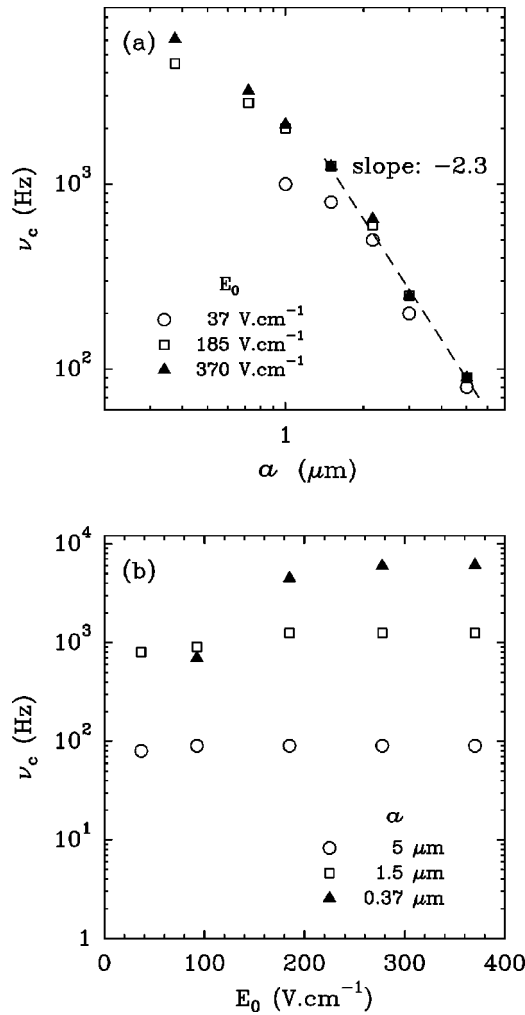


FIG. 5. Contact frequency  $\nu_c$ : (a) as a function of the particle radius  $a$  for three different  $E_0 = V_o/L$ , and (b) as a function of  $E_0$  for three different radius values.

of  $\nu_c$  on the beads radius: the smaller the particles, the higher  $\nu_c$ . In other words larger particle systems have to be submitted to lower frequency fields to undergo aggregation. A remarkable fact is that at a fixed radius  $a$ ,  $\nu_c$  seems to be almost independent of  $V_o$ , except for low values of this parameter ( $V_o < 74 \text{ V cm}^{-1}$ ) and small radii ( $a < 1 \mu\text{m}$ ). For large particles, the decrease of  $\nu_c$  with  $a$  is approximately fitted by a power law with an exponent  $\sim -2.3$ .

Intuitively, one might expect the particle surface charge density  $\sigma_s$  to be a key parameter in the aggregation phenomenon. We experimentally found that it is not. This conclusion is supported by the data of Table I. This table displays the values of  $\nu_c$  that we obtained for particles of the same size,  $a \sim 1.5 \mu\text{m}$ , but of different  $\sigma_s$ . As we had no means of determining directly  $\sigma_s$ , we measured the particles' zeta-potential  $\zeta$ , for each batch. Note that  $\zeta$  varied by an order of magnitude among the different batches. Clearly, there is no appreciable dependence of  $\nu_c$  on  $\zeta$ . In other words, the surface charge of the particle does not significantly influence the aggregation process.

In summary, the above description of the collective be-

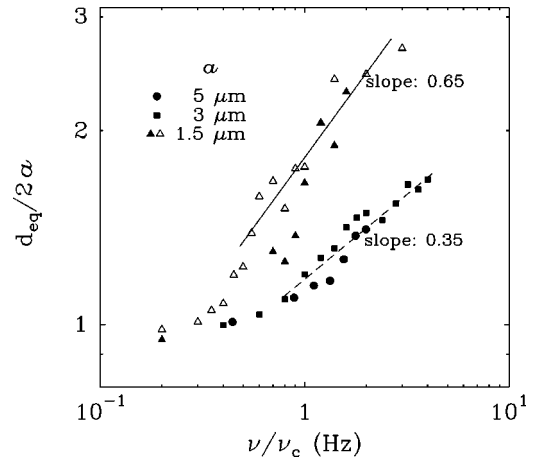


FIG. 6. Equilibrium distance between two particles as a function of the frequency, normalized by the collective contact frequency  $\nu_c$ , for three particles radii.  $E_0 = 185 \text{ V cm}^{-1}$ .  $\nu_c = 1250 \text{ Hz}$  for  $a = 1.5 \mu\text{m}$  ( $\nu_c = 250 \text{ Hz}$  for  $a = 3 \mu\text{m}$ , and  $\nu_c = 90 \text{ Hz}$  for  $a = 5 \mu\text{m}$ ).

havior points out the occurrence of a characteristic frequency  $\nu_c$  that delimits two regimes (LF and HF). When increasing progressively the frequency, from LF to HF, we observed a progressive increase of the average distance between neighboring particles. This strongly suggests the process is ruled by two antagonist forces (a repulsive one and an attractive one), that scale differently with the frequency (the attraction dominates at low frequencies, while at high frequencies the repulsion is stronger). The fact that the contact frequency does not depend on  $V_o$  suggests that both the attraction and the repulsion are induced by the ac field and scale in the same way with the field amplitude.

#### IV. TWO-PARTICLE BEHAVIOR

The essential features of the aggregation mechanism described above should be understandable on the basis of a particle pair interaction. To elucidate the nature of these interactions, we report in this section a set of experiments, which were performed with a double optical tweezer system [18], on a highly diluted dispersion of carboxylated latex particles ( $10^2$  particles per  $\text{cm}^3$ ).

In a first set of experiments, we determined the stationary (equilibrium) distance between two isolated particles, submitted to an ac electric field, as a function of the frequency. The trapping laser was used to drag two particles close to another in the microscope field of view, close to the bottom ITO-coated plate. Then the laser was switched off and the two particles were let free to move. We checked that the final two-particle configuration was a stable steady state one by checking its stability to small perturbations generated with the laser trap. As in the many particles system, the two-particle behavior was found reversible; once the ac electric field is turned off, the particles diffuse freely. Results obtained with three different particle radii ( $a = 1.5, 3$ , and  $5 \mu\text{m}$ ), and with  $E_0 = 185 \text{ V cm}^{-1}$ , are displayed in Fig. 6. The equilibrium distance  $d_{eq}$  between the two particles

smoothly increases with the adimensional frequency  $\nu/\nu_c$  ( $\nu_c$  is the contact frequency estimated from the collective behavior). The average slopes of the log-log plots of Fig. 6 range from 0.35 (3- and 5- $\mu\text{m}$  radius particles) to 0.65 (1.5- $\mu\text{m}$ -radius particles), although these values should be taken with care given the limited range of distances explored.

This two-particle behavior is, on the whole, very consistent with the collective processes described in the preceding section. The data in Fig. 6 indicate that the two-particle contact frequency  $\nu_c^{(2)}$  is smaller than the collective contact frequency  $\nu_c$ . This does not rule out our interpretation in terms of a pair interaction, as the equilibrium interparticle distance can depend on the number of interacting particles (it is the case for example, if attraction and repulsion had different ranges).

The second set of experiments aimed at analyzing separately the attraction and the repulsion.

We first probed the dipolar nature of the repulsive interaction, due to the electric polarization of the microspheres under ac electric field. This study was performed in the bulk, i.e., far from any surface. By means of the optical trap, it was possible to hold a couple of particles in the bulk electrolyte in a horizontal plane, at about middistance between the top and bottom surfaces of the sample cell. Each microsphere was held between two counter-propagating Argon ion laser beams, that constituted two 3D stable optical traps. In the horizontal plane, the traps acted as Hookean springs (stiffness  $\sim 1 \text{ pN } \mu\text{m}^{-1}$ ). When the ac voltage was turned on, the interparticle distance increased, revealing a repulsion. In this configuration, the particles got polarized by the electric field, and bore parallel electric dipoles. In this geometry, the dipole vector  $\vec{\mu}$  is perpendicular to the line linking the particle centers and the dipole-dipole interaction is repulsive. This is what the experiment confirmed whatever the frequency of the applied field (for  $\nu > \nu_c$  and  $\nu < \nu_c$ ). At this step, we can already deduce that the attraction intrinsically depends on the proximity of the conducting plate, as none was found in bulk.

Unfortunately, the configuration with the two particles repelling each other in the same horizontal plane was highly unstable, as they rapidly tended to turn around each other to align on a vertical. Because of this difficulty, it was not possible to make the observation quantitative, i.e., to measure the amplitude of the repulsion.

In order to quantitatively characterize the interaction, we instead chose to work in a configuration with  $\vec{\mu}$  parallel to the line linking the particle centers. This was achieved inside a different cell, whose structure is sketched in Fig. 7(a). Two platinum wire electrodes (diameter 0.5 mm and length 3 cm) were placed at a given distance (270  $\mu\text{m}$ ) inside a glass cell of rectangular cross section (thickness 1 mm, width 1 cm, length 3.5 cm), filled with the NaOH electrolyte ( $10^{-4} \text{ mol l}^{-1}$ ). The experiments were carried out with large particles, 5  $\mu\text{m}$  in radius, because these were hardly Brownian and still small enough to be manipulated with a moderate laser power. As soon as the potential difference is switched on, the two particles symmetrically shifted from their initial

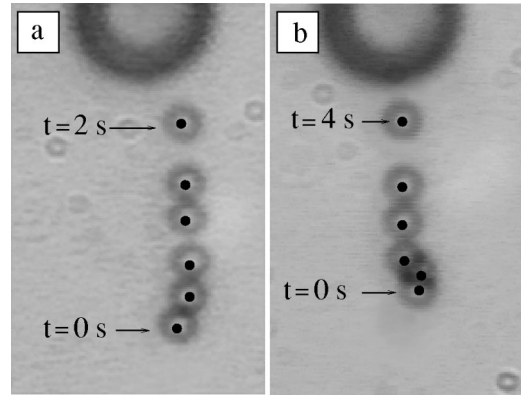


FIG. 7. Visualization of the centripetal flow in the neighborhood of a large particle ( $a=5 \mu\text{m}$ ) under ac electric field  $E_o = 185 \text{ V cm}^{-1}$ . The flow is traced by a small particle ( $a=1 \mu\text{m}$ ). On each panel the small tracer images are superimposed, for fixed time intervals  $\Delta t$ . (a)  $\nu=150 \text{ Hz}$ ,  $\Delta t=0.4 \text{ s}$ . (b)  $\nu=600 \text{ Hz}$ ,  $\Delta t=0.8 \text{ s}$ .

positions, as shown in Fig. 7(b), to quasi-instantaneously reach two new equilibrium positions (gray particles). As expected from electrostatics, the interaction in this configuration was attractive. At a fixed final distance (after shifting)  $d \sim 2.2a$  between the particle centers, for  $E_o = 185 \text{ V cm}^{-1}$  and  $\nu = 1 \text{ kHz}$ , the value of the measured attractive force was 1.2 pN. The attraction scaled as a power law in  $E_o$  ( $\sim E_o^{1.9}$ ).

The variation of this attractive force with the distance between the particles centers  $d$  could be reasonably fitted by a power law with exponent  $\sim -4.7$ , for the limited range of  $d$  between  $2a$  and  $4a$  (data not shown here, for more details see Ref. [19]).

To obtain an estimation of the expected force magnitude take two dielectric spheres of radius  $a$  and dielectric constant  $\epsilon_l$  embedded in a medium of dielectric constant  $\epsilon_w \epsilon_o$ , submitted to a slowly oscillating field  $E(t) = E_o \cos(2\pi\nu t)$  along the axis linking the centers [same configuration as on Fig. 7(a).] For  $\epsilon_w \gg \epsilon_l$ , each sphere alone would acquire an instantaneous electric dipolar moment  $\mu = 2\pi\epsilon_w \epsilon_o E(t) a^3$ . Estimating the resulting dipole-dipole force by averaging over a period, we get an order of magnitude estimate of the attractive force  $F_e^{(a)} \approx 3\pi\epsilon_o \epsilon_w a^6 E_o^2 / d^4$ , where the superscript<sup>(a)</sup> refers to the attractive configuration. Taking  $\epsilon_w \sim 80$ ,  $d \sim 10 \mu\text{m}$  and  $E_o \sim 185 \text{ V cm}^{-1}$  leads to a force around 3 pN, of the same order as the experimental measure. Moreover, the scaling law  $\sim E_o^2$  for  $F_e^{(a)}$  extracted from the experiments are in line with the above formula. We can therefore anticipate that a repulsive dipole-dipole interaction  $F_e$  must exist between two particles in the vicinity of the conducting plane (original configuration). From simple geometry this repulsion should persist in the vicinity of the conducting plane although image effects should modify its amplitude.

Second, we tried to characterize the attraction by analyzing how a 1- $\mu\text{m}$ -radius particle was attracted by an isolated larger particle of radius 5  $\mu\text{m}$ , when released at some distance from the latter. Figure 8 shows the superimposed posi-

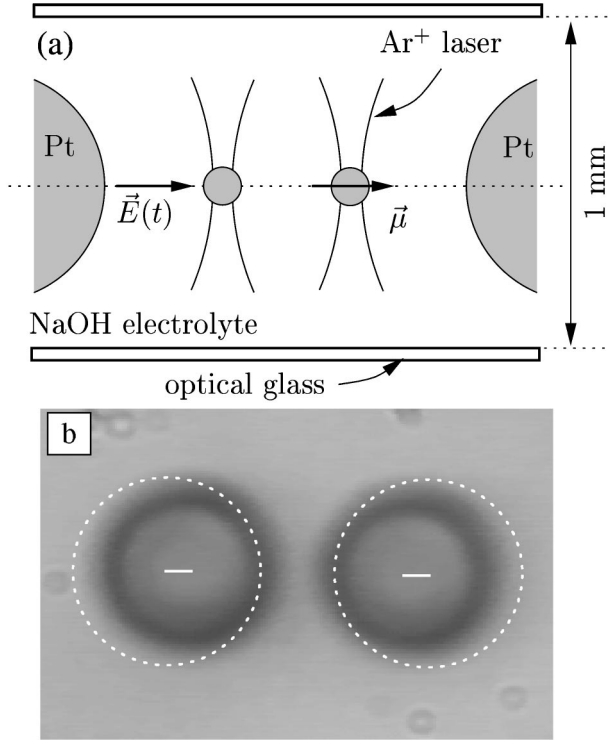


FIG. 8. Experimental evidence of the dipolar interaction between two colloidal particles submitted to an ac electric field. (a) Sketch of cell geometry. The gap between the platinum wires is about  $270 \mu\text{m}$ . The curved lines across the particles are a symbolic representation of the laser beams. (b) Visualization of the attraction between two big latex particles ( $a=5 \mu\text{m}$ ), under ac electric field ( $E_o=185 \text{ V cm}^{-1}$ ,  $\nu=1 \text{ kHz}$ ). The initial particle positions (prior to applying the voltage difference) are indicated by their contours in white dashed lines. The photos correspond to the particles final positions.

tions of the two particles taken at fixed time interval (0.4 s and 0.8 s) for  $E_o=185 \text{ V cm}^{-1}$  and two frequencies,  $\nu=150 \text{ Hz}$  (a) and  $\nu=600 \text{ Hz}$  (b). These two frequencies are located above the two-particle contact frequency of the large particle ( $\nu_c^{(2)} \sim 50 \text{ Hz}$  for  $a=5 \mu\text{m}$ ). The large particle did not move significantly during the course of the experiment. Both particle trajectories presented in Fig. 8 show that the small particle moved faster as it got closer to the larger particle. This motion was observed to be slower for larger frequencies or smaller amplitude of the ac electric field. We attempted to quantify this attractive drift by measuring the small bead velocity  $u(\nu, d)$  from the video films, at a fixed distance  $d=10 \mu\text{m}$  from the large particle center. For instance, at fixed  $E_o=185 \text{ V cm}^{-1}$ , this velocity decreased monotonically with frequency:  $u=10.4 \mu\text{m s}^{-1}$  at 150 Hz,  $u=7.8 \mu\text{m s}^{-1}$  at 300 Hz,  $u=5.3 \mu\text{m s}^{-1}$  at 600 Hz, and  $u=1 \mu\text{m s}^{-1}$  at 1.2 kHz. Following Ref. [16] it is tempting to consider the small particle as a tracer placed in an electrically induced centripetal flow around the big particle [16]. Using even smaller bitumen tracers ( $0.4 \mu\text{m}$  radius) in the vicinity of the same  $5 \mu\text{m}$  radius particles, we observed recirculation rolls that confirmed the very probable hydrodynamic nature of the attraction.

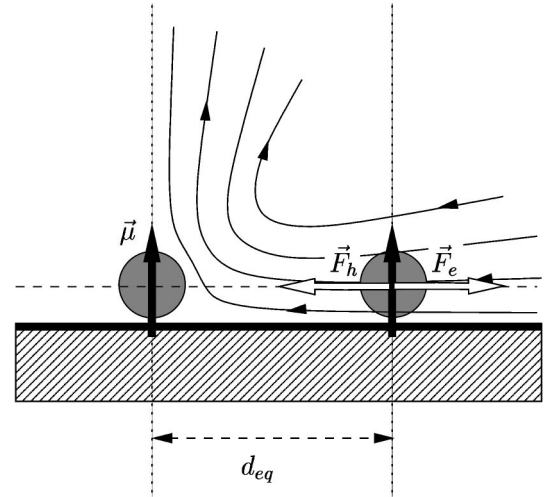


FIG. 9. Sketch of the two main forces acting on a particle. In this representation, the right bead is dragged by the flow generated by the left one. The resulting hydrodynamic force  $\vec{F}_h$  is balanced by the electrostatic repulsion  $\vec{F}_e$  between the dipoles  $\vec{\mu}$ .

Thus, to estimate the strength of the attraction between two *identical* particles, a simple picture is to consider one particle submitted to a drag force due to the flow generated by the other one (this argument breaks the symmetry but allows a first simplification). The centripetal hydrodynamic drag force  $F_h$  can be further approximated by  $F_h \sim 6\pi\eta a u(\nu, d)$ , with  $u(\nu, d)$  the frequency dependent fluid velocity at a given distance  $d$  from one of the particles, and  $\eta$  the water viscosity ( $\eta=10^{-3} \text{ kg m}^{-1} \text{ s}^{-1}$ ). The measured values of the small bead velocities given above allow us to roughly estimate the amplitude of this attractive force. For  $a=5 \mu\text{m}$ ,  $E_o=185 \text{ V cm}^{-1}$ , and  $d \sim 2a$ ,  $F_h$  equals 1 pN at  $\nu=150 \text{ Hz}$ , 0.7 pN at  $\nu=300 \text{ Hz}$ , 0.5 pN at  $\nu=600 \text{ Hz}$ , and 0.1 pN at  $\nu=1.2 \text{ kHz}$ .

This justifies *a posteriori* the use of small beads as tracers to visualize the flow created by a larger one, since the dipole electrostatic repulsion felt by a small bead scales as the third power of its radius whereas, the hydrodynamic drag attraction scales only linearly. As a consequence, the weak dipolar repulsion on the small particle should yield negligible correction on its velocity: as expected, the small particle is attracted even for frequencies greater than the contact frequency  $\nu_c^{(2)} \sim 50 \text{ Hz}$  of the large particle.

## V. DISCUSSION

The observations and estimates reported in the preceding section confirm the hypothesis that the aggregation phenomena can be explained by the competition between a dipole-dipole repulsion and an electrohydrodynamic attractive effect that, in the frequency regime  $\nu \sim \nu_c$  leads to the observed equilibrium distance  $d_{eq}(\nu)$  (see Fig. 9). For the particles of  $5\text{-}\mu\text{m}$  radius studied in Sec. IV, the estimated orders of magnitude of the repulsive and attractive contributions allow us to deduce that, for  $E_o=185 \text{ V cm}^{-1}$ , the ‘‘Stokes’’ force is

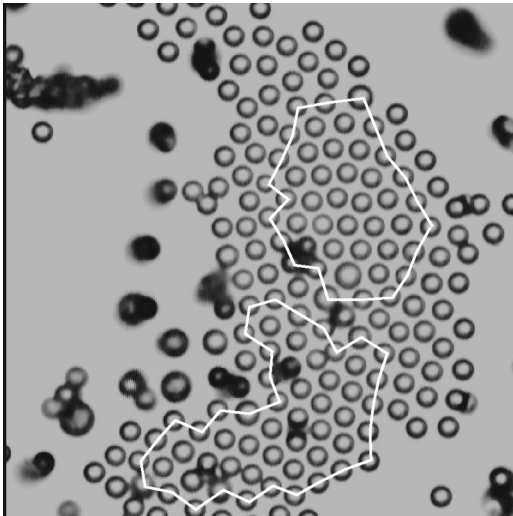


FIG. 10. Noncontact steady state structure obtained with big particles ( $a=3 \mu\text{m}$ ) at high electric field ( $E_o=560 \text{ V cm}^{-1}$ ). The frequency is 350 Hz, which is greater than  $\nu_c \sim 250 \text{ Hz}$  for this radius. The white contours have been drawn to delimit the crystalline zone with hexagonal symmetry.

able to balance the dipolar electrostatic force at low frequency ( $\nu \sim 150 \text{ Hz}$ ), while at higher frequency ( $\nu \sim 1.2 \text{ kHz}$ ), it is dominated by the electrostatic repulsion: indeed at  $\nu=1.2 \text{ kHz}$ ,  $F_h$  is lower than  $F_e$  by an order of magnitude. This not only agrees with the pattern evolution with the frequency shown in Fig. 2 but also explains the “explosion” observed when the frequency is suddenly turned up from the LF domain to the HF domain. Moreover, the fact that  $\nu_c$  is independent of  $E_o$  suggests that the attractive and repulsive forces scale similarly with  $E_o$ .

This is in agreement with the suggestion of Yeh and co-workers [16] for the origin of the attractive electrohydrodynamic effect: the distortion of the applied electric field by the dielectric particle leads to a tangential component of the electric field over the Debye layer covering the conducting surface. This generates a rectified electro-osmotic flow, proportional to both the charge in the Debye layer (which is proportional to  $E_o$  to first order), and to the tangential electric field component just outside the Debye layer (which is also proportional to  $E_o$ ). This flow (and the associated “Stokes” force) has thus the same power law dependence,  $E_o^2$ , as the dipole-dipole repulsion.

We have not attempted any more precise discussion of the exponents indicated on Figs. 5 and 6 given the limited range of values for  $d/a$  and the difficulty to build more accurate models for situations where this parameter is only barely larger than 1.

The above discussion suggests that the main features of the aggregation behavior of latex particles under ac electric field can be understood as the outcome of the sole competition between two deterministic forces (electrostatic and hydrodynamic). However, an important remark remains to be made. Turning back to Fig. 5(b), we notice a decrease of  $\nu_c$  at small values of  $E_o$  for small radii. Two points are even missing on Fig. 5(a), (for  $E_o=37 \text{ V cm}^{-1}$ ) and one on Fig. 5(b), (for  $a=0.37 \mu\text{m}$ ). For these values of the parameters, it was not possible to form even “liquid” aggregates, the Brownian motion competing against the other interactions so that the electrically induced effects were blurred by the thermal noise. Comparing the dipole-dipole repulsion for  $E_o \sim 74 \text{ V cm}^{-1}$  and  $d \sim 2a$ , to  $k_B T/a$  leads to a limit radius of  $1 \mu\text{m}$  under which the thermal noise cannot be neglected. This also explains the fact that for low voltages and small particle radius, when  $\nu$  is slightly above  $\nu_c$ , the areas covered by beads do not exhibit noncontact crystalline structure [Figs. 2(b) and 2(c)]. On the contrary, for larger particles and higher voltages, thermal agitation appeared negligible compared to the electrically induced forces, which allowed us to observe noncontact crystalline structures (see, e.g., Fig. 10).

## VI. CONCLUSION

We have presented an experimental study of the ac electric field induced aggregation of latex particles on a conducting surface, as a function of the field parameters (strength and frequency) and of the particle size and surface charge. The reported set of experimental measurements strongly suggests that the 2D organization of the particles, both in the aggregated and low-density phases, results from the competition between an electrohydrodynamic attraction and an electrostatic dipolar repulsion. Moreover, the collective aggregation behavior can be semi quantitatively understood in terms of two-particle interactions, summed up on large aggregates. The transition from 2D low-density phases to compact hexagonal aggregates can be viewed as a continuous out-of-equilibrium transition involving the competition of attractive and repulsive forces whose range and strength is changing continuously with the field frequency and amplitude. Thermal noise here only contributed to blur this electrically induced scenario for the smallest particles ( $< 1 \mu\text{m}$ ).

## ACKNOWLEDGMENTS

We are very indebted to C. Ybert and S. Ravaine for fruitful discussion. This work was supported by the Centre National des Etudes Spatiales under Grant Nos. 793/CNES/99/7725 and 793/CNES/01/503539.

- [1] M. Smoluchowski, *Bull. Int. Acad. Sci. Cracovie* **3**, 182 (1903).  
 [2] M. V. Smoluchowski, *Z. Phys. Chem., Stoechiom. Verwandschaftsl.* **92**, 129 (1917).

- [3] R. Hunter, *Foundation of Colloid Science* (Clarendon Press, Oxford, 1986), and references therein.  
 [4] J. Israelachvili, *Intermolecular and Surface Forces*, 2nd ed. (Academic Press, London, UK, 1991).

- [5] P. Pieranski, Phys. Rev. Lett. **45**, 569 (1980).
- [6] G. Onoda, Phys. Rev. Lett. **55**, 226 (1985).
- [7] A. Hurd and D. Schaefer, Phys. Rev. Lett. **54**, 1043 (1985).
- [8] G. Ye *et al.*, Phys. Rev. Lett. **81**, 622 (1998).
- [9] K. N. P. A. Kralchevsky, Adv. Colloid Interface Sci. **85**, 145 (2000).
- [10] M. Trau, D. Saville, and I. Aksay, Science **272**, 706 (1996).
- [11] M. Bohmer, Langmuir **27**, 5747 (1996).
- [12] Y. Solomentsev, M. Bohmer, and J. Anderson, Langmuir **13**, 6058 (1997).
- [13] R. Hayward, D. Saville, and I. Aksay, Nature (London) **404**, 56 (2000).
- [14] P. Richetti, J. Prost, and P. Barois, J. Phys. (France) Lett. **45**, 1137 (1984).
- [15] M. Giersig and P. Mulvaney, J. Phys. Chem. **97**, 6334 (1993).
- [16] S. Yeh, M. Seul, and B. Shraiman, Nature (London) **386**, 57 (1997).
- [17] B. P. M. I. Angelova, Pure Appl. Opt. **2**, 261 (1993).
- [18] G. Martinot-Lagarde *et al.*, Pure Appl. Opt. **4**, 571 (1995).
- [19] F. Nadal *et al.* (unpublished).